Handout # 14 (MEEN 626) **Application example**

Experimental identification of bearing force coefficients

Experimental identification of the dynamic force coefficients of bearings, seals and other rotor support elements is of importance (a) to predict, at the design stage, the dynamic force performance of a rotor using these elements; (b) to reproduce rotordynamic performance when troubleshooting rotor-bearing system malfunctions or searching for instability sources; and (c) to validate (and calibrate) predictive tools for bearing and seal analyses. The ultimate goal is to collect e a reliable data base from which to determine the confidence of bearing and/or seal operation under both normal design conditions and extreme environments due to unforeseen events.

In addition, even advanced predictive computational physics based models are very limited or non-existing for certain bearing and seal configurations and with stringent particular operating conditions, and thus experimental measurement of the actual element force coefficients constitute the only option available to generate engineering results of interest. Squeeze film dampers operating with persistent air ingestion and entrapment are an application example where systematic experimentation becomes mandatory.

The widespread availability and low-cost of PC high-speed data acquisition equipment and (real time) data signal processing have promoted dramatic advancements in the field of bearing and seal parameter identification. In most cases, methods are restricted to the laboratory environment and strictly applicable to rigid rotor configurations and identical bearing supports. Time and frequency

domain based parameter identification procedures are based on the seminal works of Goodwin [1991] and Nordmann [1980], respectively.

Tiwari, R., Lees, A.W., Friswell, M.I. 2004. "Identification of Dynamic Bearing Parameters: A Review." *The Shock and Vibration Digest*, **36,** pp. 99-124.

The paper reviews the most popular test techniques and analysis methods to identify linearized force coefficients in fluid film bearings. The methods include time and frequency domain procedures, while experimentation focuses on the types of dynamic load excitation most efficient for a particular procedure. The review also includes physics based mathematical modeling with governing equations of the test bearing element or rotor-bearing system, parameter extraction algorithms, and uncertainty in the estimates. The classification of identification techniques is based on the method used to excite the test element or system: short duration (impacts and shock loads), periodic load excitation, fixed or sine-sweep and including imbalance induced forces, and random load excitation techniques.

Identification algorithms consider the test bearing or support as a two degree of freedom mechanical system undergoing lateral motions $(x,\ y)_{(t)}$ and with readily available (measured) support transmitted forces and rotor displacements from which test impedances or mobilities are obtained. Curve fits to the appropriate transfer functions give the support mechanical parameters.

For lateral rotor motions (x, y), a bearing or seal reaction force vector $\mathbf{f}$ is usually modeled as

$$\begin{bmatrix} f_{X_{(t)}} \\ f_{Y_{(t)}} \end{bmatrix} = \begin{bmatrix} f_{Xo} \\ f_{Yo} \end{bmatrix} - \begin{bmatrix} K_{XX} & K_{XY} \\ K_{YX} & K_{YY} \end{bmatrix} \begin{bmatrix} X_{(t)} \\ Y_{(t)} \end{bmatrix} - \begin{bmatrix} K_{XX} & K_{XY} \\ K_{YX} & K_{YY} \end{bmatrix} \begin{bmatrix} x_{(t)} \\ y_{(t)} \end{bmatrix} - \begin{bmatrix} C_{XX} & C_{XY} \\ C_{YX} & C_{YY} \end{bmatrix} \begin{bmatrix} \dot{x}_{(t)} \\ \dot{y}_{(t)} \end{bmatrix} - \begin{bmatrix} M_{XX} & M_{XY} \\ M_{YX} & M_{YY} \end{bmatrix} \begin{bmatrix} \ddot{x}_{(t)} \\ \ddot{y}_{(t)} \end{bmatrix} \tag{1.1}$$

or

$$\mathbf{f}_{(t)} = \begin{bmatrix} \mathbf{f_X} \\ \mathbf{f_Y} \end{bmatrix} = \mathbf{f_o} - \mathbf{K}\,\mathbf{x} - \mathbf{C}\,\dot{\mathbf{x}} - \mathbf{M}\,\ddot{\mathbf{x}} \quad \text{with} \quad \mathbf{x}_{(t)} = \begin{bmatrix} x \\ y \end{bmatrix} \tag{1.2}$$

where $\mathbf{f_o}$ is a static equilibrium force typically counteracting a fraction of the rotor weight, for example. The test element force coefficients are four (4) stiffness K and four (4) damping C force coefficients in mineral oil lubricated bearings, oil seals, and also gas damper seals. In liquid annular (damper) seals and bearings (hydrostatic and/or hydrodynamic) working with process fluids (water or LOx, for example), four (4) inertia force coefficients M are also important.

Please note that these force coefficients (K, C, M) are mechanical parameters representative of a **linear or** rather **linearinzed physical system.** In this regard, the (K, C, M) coefficients are to be determined in a system or test element undergoing small amplitude motions about an equilibrium condition. This operating condition is of utmost importance to obtain reliable and repeatable results. Unfortunately, the basic assumption – needed to ensure the physical model is linear- is

often not considered by the experimenters, and which explains the vast differences in parameter magnitudes when compared to analytical model predictions, for example.

Incidentally, the linearized coefficient model for the test element, i.e. a bearing or a seal or a support, also assumes that the **coefficients are frequency independent**. Only in the last 10 years, since the late 1990's, the engineering community has recognized this limitations and developed techniques to extract parameters from frequency domain measurements.

Furthermore, note that the so called "experimental" force coefficients (*K, C, M*) are in actuality not measured parameters but mere ESTIMATIONS derived from procedures (ranging from simple or complex) that relate motions of the test system or element due to known applied forces.

Until recently, estimation of bearing and seal rotordynamic force coefficients was traditionally based on time domain response methods. These techniques, often limited in scope, use only a limited amount of the recorded information rendering poor results with marginal confidence levels. **Modern parameter identification techniques** are based on **frequency domain procedures**, where dynamic force coefficients are estimated from **transfer functions of measured** displacements (velocities and accelerations as well) due to **external loads of a prescribed time varying structure.** Frequency domain methods take advantage of high speed computing and digital signal processors, thus producing estimates of system parameters in real time and at a fraction of the cost (and effort) with cumbersome time domain algorithms.

Consider a test bearing or seal element as a point mass undergoing forced vibrations induced by external forcing functions.

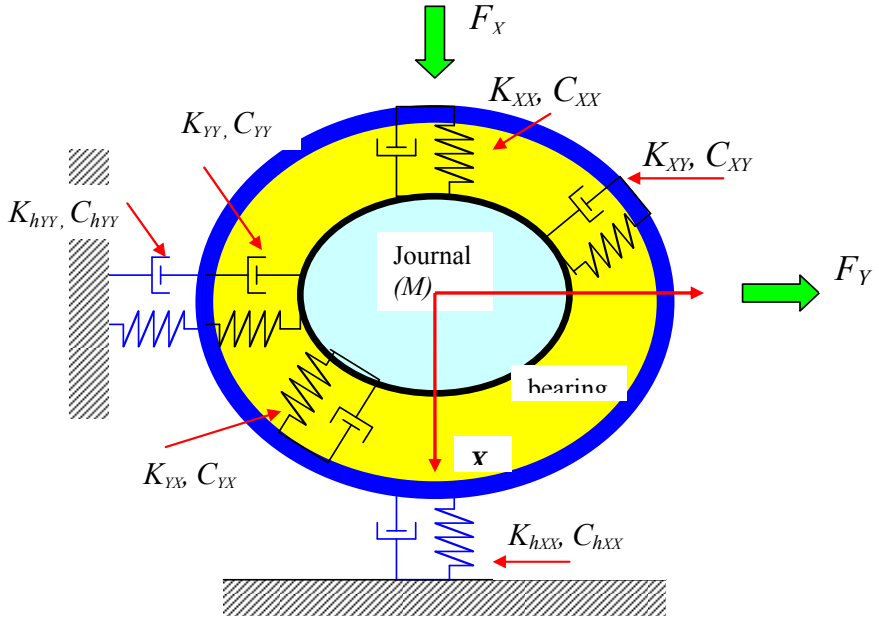

Representation of point mass and bearing force coefficients used for identification of parameters from dynamic load and motion measurements

For small amplitudes about an equilibrium position, the equations of motion of a linear mechanical system are

$$M_h\ddot{x} + \left(C_{XX} + C_{hX}\right)\dot{x} + C_{XY}\dot{y} + \left(K_{XX} + K_{hX}\right)x + K_{XY}y = f_X$$

$$M_h\ddot{y} + \left(C_{YY} + C_{hY}\right)\dot{y} + C_{YX}\dot{x} + \left(K_{YY} + K_{hY}\right)y + K_{YX}x = f_Y \qquad (2)$$

where

$\{f_i\}_{i=X,Y}$	external excitation forces,
M_h	test element mass,
$\{K_{hi},\ C_{hi}\}_{i=X,Y}$	(any) structural support stiffness and remnant damping coefficients[1], and
$\{K_{ij},\ C_{ij}\}_{i,j=X,Y}$	seal or bearing dynamic stiffness and damping force coefficients.

Inertia force coefficients are not included in the model above. Added mass coefficients are NOT significant, i.e. their magnitude is small, for highly compressible fluids (LH_2 or gases) and in most bearing and seals lubricated with mineral oil[2]. The apparent simplification is easily removed and does not diminish the importance of the identification method. The test system structural stiffness and damping coefficients, $\{K_{hi}, C_{hi}\}_{i=X,Y}$, are obtained from prior shake tests results under dry conditions, i.e. without fluid through the test element

Two independent force excitations (impact, periodic-single frequency, sine-swept, random, etc) $(f_X, 0)^T$ and $(0, f_Y)^T$, for example, are applied to the test element. This process is formulated as

1. Apply $\begin{bmatrix} f_{x_1} \\ f_{y_1} \end{bmatrix}_{(t)}$ and measure $\begin{bmatrix} x_{1_{(t)}} \\ y_{1_{(t)}} \end{bmatrix}$ (3a); apply $\begin{bmatrix} f_{x_2} \\ f_{y_2} \end{bmatrix}_{(t)}$ and measure $\begin{bmatrix} x_{2_{(t)}} \\ y_{2_{(t)}} \end{bmatrix}$ (3b)

[1] Refers to any mechanical component assisting to support the test bearing, for example connecting rods or springs; and damping from the test system DRY, i.e. without any lubricant, for example.

[2] Note that test data by Childs et al. obtained for mineral oil tilting pad bearings, pressure dam bearings and floating ring seals actually evidence these test elements show large added mass coefficients; larger in magnitude than theoretical model predictions. See Notes 7 or Notes 11 for further details and discussion.

2. Obtain the **discrete Fourier transform (DFT)**[3] of the applied forces and displacements, i.e. Let

$$\begin{bmatrix} F_{X_{1(\omega)}} \\ F_{Y_{1(\omega)}} \end{bmatrix} = DFT \begin{bmatrix} f_{x_{1(t)}} \\ f_{Y_{1(t)}} \end{bmatrix}; \begin{bmatrix} X_{1(\omega)} \\ Y_{1(\omega)} \end{bmatrix} = DFT \begin{bmatrix} x_{1(t)} \\ y_{1(t)} \end{bmatrix}; \tag{4a}$$

$$\begin{bmatrix} F_{X_{2(\omega)}} \\ F_{Y_{2(\omega)}} \end{bmatrix} = DFT \begin{bmatrix} f_{x_{2(t)}} \\ f_{Y_{2(t)}} \end{bmatrix}; \begin{bmatrix} X_{2(\omega)} \\ Y_{2(\omega)} \end{bmatrix} = DFT \begin{bmatrix} x_{2(t)} \\ y_{2(t)} \end{bmatrix} \tag{4b}$$

The DFT is an operation that transforms the information from the **time domain** into the **frequency domain**. Incidentally, recall that

$$i\,\omega\, X_{(\omega)} = DFT\left[\dot{x}_{(t)}\right]; \quad -\omega^2\, X_{(\omega)} = DFT\left[\ddot{x}_{(t)}\right] \tag{5}$$

---

[3] A sequence of *N* time-domain data points, say $[(z_1,t_1=0), (z_2,t_2), \ldots. (z_N,t_N=t_{max})]$ and with $\Delta t=t_2-t_1= t_3-t_2=\ldots$, will transform, using the DFT algorithm, into ½ *N* coefficients (complex numbers with amplitude and phase) at discrete frequencies $Z_k=a_k e^{i\phi_k}$ at discrete frequencies $\omega_0=0$, $\omega_1=\delta_\omega$, $\omega_2=2\delta_\omega$,….. $\omega_{N/2}=½\ N\ \delta_\omega= \omega_{max}= 1/(2\Delta t)$. Hence, $\delta_\omega=1/(N\ \Delta t) \sim 1/t_{max}$. Typically, *N* is a power of 2, i.e. *N*=256, 512, etc for efficient and fast data processing. Note that $1/\Delta t$ is known as the **sampling rate.** In addition, **the longer the time span for analysis (t_{max}), the smaller is the frequency step (δ_ω); while the faster the data acquisition sampling rate,** Δt is small, the highest is the maximum frequency (ω_{max}) of the DFT. Satisfying both small δ_ω and very high ω_{max} may require of exceedingly large number of data points. Often, these two conditions can not be attained simultaneously; and in which case care is needed to avoid aliasing of the recorded signal as well as other spurious effects. Read a dedicated book in Fast Fourier Transform analysis for more accurate and relevant details.

3. For the **assumed** physical model, the motion ODEs become for the first test set and in the frequency domain:

$$-M_h\omega^2 X_1 + \left(C_{XX} + C_{hX}\right) i\omega X_1 + C_{XY} i\omega Y_1 + \left(K_{XX} + K_{hX}\right) X_1 + K_{XY} Y_1 = F_{X_1}$$

$$-M_h\omega^2 Y_1 + \left(C_{YY} + C_{hY}\right) i\omega Y_1 + C_{YX} i\omega X_1 + \left(K_{YY} + K_{hY}\right) Y_1 + K_{YX} X_1 = F_{Y_1} \quad (6)$$

Or, written in matrix form as

$$\begin{bmatrix} K_{XX} + K_{hX} - M_h\omega^2 + i\omega\left(C_{XX} + C_{hX}\right) & K_{XY} + i\omega C_{XY} \\ K_{YX} + i\omega C_{YX} & K_{YY} + K_{hY} - M_h\omega^2 + i\omega\left(C_{YY} + C_{hY}\right) \end{bmatrix} \begin{Bmatrix} X_1 \\ Y_1 \end{Bmatrix} = \begin{Bmatrix} F_{X_1} \\ F_{Y_1} \end{Bmatrix}$$

Define **complex impedances**[4] $\{H_{ij}\}_{i,j=X,Y}$ as

$$H_{ij} = \left[\left(K_{ij} + K_{hi}\delta_{ij}\right) - \omega^2 M_{hi}\delta_{ij}\right] + i\omega\left(C_{ij} + C_{hi}\delta_{ij}\right) \quad (7)$$

where $i = \sqrt{-1}$, $\delta_{ij} = 1$ for $i = j = X, Y$; zero otherwise.

[4] As you know well, impedance is a misnomer. Dynamic (complex) stiffness is a more appropriate name.

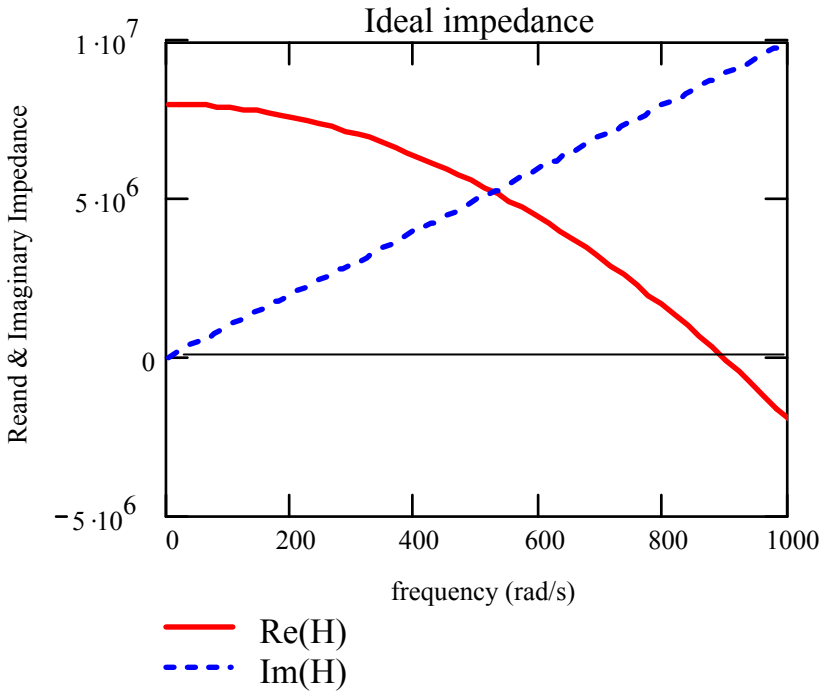

The impedances comprise real and imaginary parts, both functions of the excitation frequency (ω). The real part denotes the dynamic stiffness, while the imaginary part (quadrature stiffness) is proportional to the *viscous* damping coefficient, as shown in the figure.

xx

Real and imaginary parts of ideal mechanical impedance representative of assumed physical model

With definition (7), the EOMs (6) become, for the first & second tests,

$$\begin{bmatrix} H_{XX_{(\omega)}} & H_{XY_{(\omega)}} \\ H_{YX_{(\omega)}} & H_{YY_{(\omega)}} \end{bmatrix} \begin{Bmatrix} X_1 \\ Y_1 \end{Bmatrix} = \begin{Bmatrix} F_{X_1} \\ F_{Y_1} \end{Bmatrix} \quad \text{and} \quad \begin{bmatrix} H_{XX_{(\omega)}} & H_{XY_{(\omega)}} \\ H_{YX_{(\omega)}} & H_{YY_{(\omega)}} \end{bmatrix} \begin{Bmatrix} X_2 \\ Y_2 \end{Bmatrix} = \begin{Bmatrix} F_{X_2} \\ F_{Y_2} \end{Bmatrix} \tag{6a}$$

Add these two equations and reorganize them as

$$\begin{bmatrix} H_{XX} & H_{YX} \\ H_{XY} & H_{YY} \end{bmatrix} \begin{bmatrix} X_1 & X_2 \\ Y_1 & Y_2 \end{bmatrix} = \begin{bmatrix} F_{X_1} & F_{X_2} \\ F_{Y_1} & F_{Y_2} \end{bmatrix} \tag{8}$$

At each frequency ($\omega_{k=1,2,\ldots n}$), Eq. (8) represents **four independent equations** with **four unknowns**, $(H_{XX}, H_{YY}, H_{XY}, H_{YX})$. Hence,

$$\begin{bmatrix} H_{XX} & H_{YX} \\ H_{XY} & H_{YY} \end{bmatrix} = \begin{bmatrix} F_{X_1} & F_{X_2} \\ F_{Y_1} & F_{Y_2} \end{bmatrix} \begin{bmatrix} X_1 & X_2 \\ Y_1 & Y_2 \end{bmatrix}^{-1} \tag{9a}$$

$$\mathbf{H} = \begin{bmatrix} \mathbf{F}^{(1)} & \mathbf{F}^{(2)} \end{bmatrix} \begin{bmatrix} \mathbf{X}^{(1)} & \mathbf{X}^{(2)} \end{bmatrix}^{-1} \quad \text{where} \quad \mathbf{F}^{(1)} = \begin{bmatrix} F_{X_1} \\ F_{Y_1} \end{bmatrix} \& \ \mathbf{X}^{(1)} = \begin{bmatrix} X_1 \\ Y_1 \end{bmatrix}, \ \mathbf{F}^{(2)} = \begin{bmatrix} F_{X_2} \\ F_{Y_2} \end{bmatrix} \& \ \mathbf{X}^{(2)} = \begin{bmatrix} X_2 \\ Y_2 \end{bmatrix} \tag{9b}$$

The **meaning of linear independence** of the test forces (and ensuing motions) should now be clear. That is, the forces in the second test cannot be a multiple of the first set of forces since then, both the matrix of forces $[\mathbf{F}^{(1)}\ \mathbf{F}^{(2)}]$ and the matrix of ensuing displacements $[\mathbf{X}^{(1)}\ \mathbf{X}^{(2)}]$ become **singular**.

The experimenter must select sets of excitations that are linearly independent, for example $(f_X, 0)^T$ and $(0, f_Y)^T$ are preferred (and easy) choices.

In the identification process, the importance of linear independence in the application of forces and ensuing test system or bearing displacements is MOST important to obtain reliable and

repeatable results. In actual practice, measured displacements may not appear similar to each other but nonetheless produce an identification matrix that is ill conditioned, i.e., the determinant of matrix $\mathbf{[X^{(1)}\ X^{(2)}]}$ is close to zero or is zero. In this case, the **condition number of the identification matrix** is of importance to determine whether the identified coefficients are any good. Test elements that are nearly isotropic and that are excited by periodic (single frequency) loads producing circular orbits of the test system usually determine a too *ill conditioned* system (Murphy, 1990).

Often enough the calculation of the matrix $\mathbf{[X^{(1)}\ X^{(2)}]}$ condition number and checking for ill-conditioning is easily overlooked.

Preliminary estimates of the system parameters $\{M,\ K,\ C\}_{i,j=X,Y}$ are determined by curve fitting of the test derived discrete set of impedances $(H_{XX},\ H_{YY},\ H_{XY},\ H_{YX})_{k=1,2....}$, one set for each frequency ω_k, to the analytical formulas over a pre-selected frequency range. That is, for example

$$\left(K_{XX}+K_{hX}\right)-\omega^2 M_h=\text{Real}\left(H_{XX}\right) \qquad \omega\left(C_{XX}+C_{hX}\right)=\text{Ima}\left(H_{XX}\right) \qquad (10)$$

Since 1993, Childs and students excel in employing the impedance identification method to "measure" rotordynamic force coefficients in hydrostatic bearings and annular seals with water as the lubricant (Rouvas and Childs, 1993). The method lends itself to simple curve-fitting of the recorded impedance functions H to physically representative analytical functions, i.e. $K\text{-}\omega^2 M$ and ωC.

Analytical curve fitting of any data renders a **correlation coefficient** (r^2) representing the goodness of the fit. A low value of the correlation coefficient, $r^2 << 1$, does not mean the test data or the obtained impedance are incorrect, but rather that the physical model (analytical function) chosen to represent the test system does not actually reproduce the measurements. On the other hand, a high $r^2 \sim 1$ demonstrates that the physical model, say with a constant stiffness K and viscous damping C in $K-\omega^2 M$ and ωC, respectively, actually describes the measurements (system response) with accuracy.

System transfer functions (output/input) are often used to obtain **more precise estimates** of the seal or bearing force coefficients (Nordmann and Schollhorn, 1980, Massmann and Nordmann, 1985). This process leads to curve fits of nonlinear functions.

Transfer functions (displacement/force) known as **test system flexibilities G** are derived as functions of the impedances, $(H_{ij})_{i,,j=X,Y}$ from the fundamental equation $\mathbf{G = H^{-1}}$, i.e.

$$G_{XX} = TF(X_1) = \frac{H_{YY}}{\Delta}; \quad G_{XY} = TF(X_2) = \frac{-H_{XY}}{\Delta}$$

$$G_{YX} = TF(Y_1) = \frac{-H_{YX}}{\Delta}; \quad G_{YY} = TF(Y_2) = \frac{H_{XX}}{\Delta} \qquad (11a)$$

where

$$\Delta = H_{XX} H_{YY} - H_{XY} H_{YX} \qquad (11c)$$

Next, the **Instrumental Variable Filter (IVF) method** of Fritzen (1985), an extension of a **least-squares estimation** method, is used to simultaneously curve fit all four transfer functions from motion measurements due to two sets of (linearly independent) applied loads. **The IVF method has the advantage of eliminating bias typically seen in an estimator due to measurement noise.**

The product of the flexibility (**G**) and impedance (**H**) matrices should be identically equal to the identity matrix $\mathbf{I}=\begin{bmatrix}1 & 0\\ 0 & 1\end{bmatrix}$ since $\mathbf{G}=\mathbf{H}^{-1}$.

However, in any measurement process there is some noise associated with the experiments. Thus, an **error matrix** (**e**) is introduced into the fundamental relationship,

$$\mathbf{G}\cdot\mathbf{H}=\mathbf{G}\left[\mathbf{K}-\omega^2\mathbf{M}+i\,\omega\mathbf{C}\right]=\mathbf{I}+\mathbf{e} \qquad (12)$$

where **K, C** and **M** are matrices of system stiffness, damping and added mass coefficients.

$$\mathbf{K}=\begin{bmatrix}K_{XX}+K_{hX} & K_{XY}\\ K_{YX} & K_{YY}+K_{hY}\end{bmatrix},\mathbf{C}=\begin{bmatrix}C_{XX}+C_{hX} & C_{XY}\\ C_{YX} & C_{YY}+C_{hY}\end{bmatrix},\ \mathbf{M}=\begin{bmatrix}M_{XX}+M_{h} & M_{XY}\\ M_{YX} & M_{YY}+M_{h}\end{bmatrix}$$

For generality, added mass coefficients (M_{XX}, M_{YY}, M_{XY}, M_{YX}) are included in the matrices above.

In Eq. (12) **G** denotes the **measured flexibility matrix** while **H** represents the (to be) estimated test system impedance as defined in Eq. (7). **Recall that Eq. (7) corresponds to the physical model ASSUMED to best represent the test system or test element.**

In the present method, the flexibility coefficients (**G**) work as weight functions of the errors in a minimization procedure. Whenever the flexibility coefficients are large, the error is also penalized by a larger value. As a result, the minimization procedure will become better in the neighborhood of the system resonances (natural frequencies) where the dynamic flexibilities are maxima (i.e., null dynamic stiffness, $(K-\omega^2 M)=0$. That is, the measurements containing resonance regions will have more weight on the fitted system parameters. External forcing functions exciting the test system resonances are more reliable because at those frequencies the system is more sensitive, and the measurements are accomplished with larger signal to noise ratios.

In addition, it is precisely around the resonant frequencies where all the physical parameters (mass, damping and stiffness) most affect appreciably the system response. For "too low" frequencies the important parameter is the stiffness, while for "too high" frequencies the inertia dominates the response. Only near the resonance do all three parameters have an important effect on the system amplitude response.

Therefore, it is **more accurate to minimize the approximation errors** using Eq. (12) rather than directly curve fitting the impedances, i.e. simply using Eq. (10). Unfortunately, the process is not straightforward and leads to a rather complex minimization scheme.

Write the impedance matrix $\mathbf{H}$ representing the test system or test element as

$$\mathbf{H}_{(\omega)} = \left[-\omega^2 \mathbf{I} \,\vdots\, i\,\omega \mathbf{I} \,\vdots\, \mathbf{I} \right] \begin{bmatrix} \mathbf{M} \\ \mathbf{C} \\ \mathbf{K} \end{bmatrix} \tag{14}$$

with $i = \sqrt{-1}$ and $\mathbf{I} = \begin{bmatrix} 1 & 0 \\ 0 & 1 \end{bmatrix}$. Thus Eq. (12) becomes at each discrete frequency $\omega_{k=1,2\ldots,n}$

$$\mathbf{G}^k \left[-\omega_k^2 \mathbf{I} \,\vdots\, i\,\omega_k \mathbf{I} \,\vdots\, \mathbf{I} \right] \begin{bmatrix} \mathbf{M} \\ \mathbf{C} \\ \mathbf{K} \end{bmatrix} = \mathbf{I} + \mathbf{e}^k \tag{15a}$$

Let

$$\mathbf{A}^k = \mathbf{G}^k \left[-\omega_k^2 \mathbf{I} \,\vdots\, i\,\omega_k \mathbf{I} \,\vdots\, \mathbf{I} \right] \tag{16}$$

And write Eq. (15a) as

$$\mathbf{A}^k \begin{bmatrix} \mathbf{M} \\ \mathbf{C} \\ \mathbf{K} \end{bmatrix} = \mathbf{I} + \mathbf{e}^k \tag{15b}$$

Now, stack all the equations, one for each frequency $\omega_{k=1,2\ldots,n}$, to obtain the set

$$\underline{\mathbf{A}} \begin{bmatrix} \mathbf{M} \\ \mathbf{C} \\ \mathbf{K} \end{bmatrix} = \underline{\mathbf{I}} + \underline{\mathbf{e}} \tag{17}$$

where $\underline{\mathbf{A}} = \begin{bmatrix} \mathbf{A}^1 \\ \mathbf{A}^2 \\ \mathbf{A}^n \end{bmatrix}$, $\underline{\mathbf{e}} = \begin{bmatrix} \mathbf{e}^1 \\ \mathbf{e}^2 \\ \mathbf{e}^n \end{bmatrix}$ and $\underline{\mathbf{I}}^T = \begin{bmatrix} 0 & 1 & 0 & 1 & 0 & 1 & .. & .. & .. & .. & 0 & 1 \\ 1 & 0 & 1 & 0 & 1 & 0 & .. & .. & .. & .. & 1 & 0 \end{bmatrix}$ (18)

$\underline{\mathbf{A}}$ contains the stack of measured flexibility functions (at discrete frequencies $\omega_{k=1,2\ldots,n}$). Eq. (17) is an over determined set of equations, i.e. there are more equations than unknowns. Hence, its **solution by least-squares aims to minimize the Euclidean norm of $\underline{\mathbf{e}}$. This minimization leads to the normal equations,**

$$\begin{bmatrix} \mathbf{M} \\ \mathbf{C} \\ \mathbf{K} \end{bmatrix} = \left(\underline{\mathbf{A}}^{\mathbf{T}} \underline{\mathbf{A}} \right)^{-1} \underline{\mathbf{A}}^{\mathbf{T}} \underline{\mathbf{I}} \tag{19}$$

A first set of force coefficients (**M,C,K**) is determined from these equations.

Fritzen (1985) introduced the elegant **Instrumental Variable Filter Method (*IVF*)** to solve the system coefficients that minimize the Euclidean (L^2) norm of the system error $\underline{\mathbf{e}}$. The IVF procedure was originally developed to estimate parameters in econometric problems. Massmann and Nordmann (1985) applied successfully the method to fluid film annular seal elements.

In the **IVF** method, the weighting function, $\underline{\mathbf{A}}$, is replaced by a new matrix function, $\underline{\mathbf{W}}$, created from the analytical flexibilities resulting from the (initial) least-squares curve fit, i.e., solution of Eq. (19). **This weighting function $\underline{\mathbf{W}}$ is free of measurement noise** and contains peaks only at the resonant frequencies as determined from the first estimates of stiffness, mass and damping force coefficients.

At step *m,*

$$\begin{bmatrix} \mathbf{M} \\ \mathbf{C} \\ \mathbf{K} \end{bmatrix}^{m+1} = \left(\left[\underline{\mathbf{W}}^m \right]^T \underline{\mathbf{A}} \right)^{-1} \left[\underline{\mathbf{W}}^m \right]^T \underline{\mathbf{I}} \tag{20}$$

where

$$\underline{\mathbf{W}}^m = \begin{bmatrix} \left[\underline{\bar{\mathbf{F}}}^m_{(\omega_1)} \left[-\omega_1^2 \mathbf{I} \mid i\omega_1 \mathbf{I} \mid \mathbf{I} \right] \right] \\ \vdots \\ \left[\underline{\bar{\mathbf{F}}}^m_{(\omega_n)} \left[-\omega_n^2 \mathbf{I} \mid i\omega_n \mathbf{I} \mid \mathbf{I} \right] \right] \end{bmatrix}$$

and

$$\underline{\bar{\mathbf{F}}}^m_{(\omega)} = \left[\left[-\omega^2 \mathbf{I} \mid i\,\omega \mathbf{I} \mid \mathbf{I} \right] \begin{bmatrix} \mathbf{M} \\ \mathbf{C} \\ \mathbf{K} \end{bmatrix}^m \right]^{-1} \tag{21}$$

A first iteration (m=1) is performed with $\mathbf{W}^1=\mathbf{A}$, which corresponds to the standard least-squares solution of the problem, eq. (19). Then, Eqs. (20) and (21) are applied iteratively until a given convergence criterion or tolerance is satisfied. This criterion can be conveniently chosen depending on the desired results. For example, the square summation of the differences between the parameters at iteration m and (m-1) can be required to be less than a certain value, i.e. limiting the Euclidean norm of the error. Alternatively, it can be required that the largest difference be less than the largest acceptable error, i.e. limiting the L_1 norm of the error. Different tolerances to each variable could also be asserted depending on their physical units and significance.

It should be clear that the substitution of $\mathbf{W}$ for the discrete measured flexibility $\mathbf{A}$ (which also contains noise) improves the prediction of the system parameters. Note that the product $\mathbf{A}^T\mathbf{A}$ amplifies the noisy components and adds them. Therefore, even if the noise has a zero mean value, the addition of its squares becomes positive resulting in a bias error. On the other hand, $\mathbf{W}$ does not have components correlated to the measurement noise. That is, no **bias error** is kept in the product $\mathbf{W}^T\mathbf{A}$. Consequently, the approximation to the system parameters is improved.

Note that the force coefficients are identified in the frequency domain. Thus, magnitudes of uncertainty for the estimated force coefficients must be obtained by comparing the original frequency responses with the frequency response of a reference excitation force and associated displacement time response. Evaluation of coherence functions then becomes necessary to reproduce the exact variability of the identified force coefficients.

Closure

Read the paper of Diaz and San Andrés (1999) – following pages- for further insight on the IVF method as applied to a *n-DOF* system. A MATHCAD® program is available for your self-study and further learning.

An example of parameter identification representative of your lecturer's research will be presented in class.

Recent developments on field or in-situ parameter identification methods

Field identification of fluid film bearing parameters is critical for adequate interpretation of rotating machinery performance and necessary to validate or calibrate predictions from restrictive computational fluid film bearing models. The key features of a successful method for ready field implementation are minimal external equipment, little or no changes to existing hardware, and the use of measuring instruments commonly used in machine protection and monitoring.

DeSantiago and San Andrés (2004, 2007) detail a simple method for estimating **in-situ** bearing support force coefficients in **flexible rotor-bearing systems**. The model neither adds mathematical complexity to existing rigid rotor models nor requires additional instrumentation than that already available in most high performance turbomachinery. The method requires two independent tests with known mass imbalance distributions and the measurement of the rotor motion (amplitude and phase) at locations close to the supports. A good rotor model (elastic and mass properties) must represent the (non observable or not measured) degrees of freedom. The procedure finds the bearing transmitted forces as a function of observable quantities (rotor motions at one side of the bearings). Imbalance response measurements conducted with a two-disk

flexible rotor supported on two-lobe fluid film bearings allow validation of the identification method estimations. Predicted (linearized) bearing force coefficients agree reasonably well with the parameters derived from the test data.

A commercial compressor company uses successfully the method advanced to qualify its equipment as per API requirements and for real-time assessment of bearing condition from measurements of rotor motions while the compressor is in operation.

Recent developments on the identification of force coefficients in non-linear systems

San Andrés and Delgado (2007-2009) have developed efficient methods to identify force coefficients in test systems that combine both linear and nonlinear mechanical elements. They apply the method to a SFD that integrates a contacting end seal to prevent air ingestion. The system motion is non-linear due to dry friction interaction at the mechanical seal mating surfaces. Single parameter characterization of the test system would yield an equivalent viscous damping coefficient that is both frequency and motion amplitude dependent. The algorithm takes the nonlinear test system as a combination of linear and nonlinear inputs with linear operators on a multiple-input/single output scheme (Rice and Fitzpatrick, 1991)

The identification method suited for nonlinear systems allows determining simultaneously the squeeze film damping and inertia force coefficients and the seal dry friction force. The identification procedure shows similar (within 10 %) force coefficients than those obtained with a more involved two-step procedure that first requires measurements without any lubricant in the test system to determine the dry-friction parameter. The identified SFD damping and inertia force coefficients agree well with model predictions that account for end flow effects at recirculation

grooves. The nonlinear identification procedure saves time and resources while producing reliable physical parameter estimations.

References

Tiwari, R., Lees, A.W., and Friswell, M.I., 2004, "Identification of Dynamic Bearing Parameters: A Review," Shock and Vibration Digest, **36**, pp. 99-124.

Nordmann, R., and Schollhorn, K., 1980, "Identification of Stiffness and Damping Coefficients of Journal Bearings by Means of the Impact Method," *Proc. Vibrations in Rotating Machinery: 2nd International Conference*, Inst. Mech. Eng., Cambridge, UK, pp. 231-238.

Goodwin, M. J., 1991, "Experimental Techniques for Bearing Impedance Measurement", *Journal of Engineering for Industry*, Vol. 113, Aug., pp. 335-342.

Murphy, B., and Scharrer, J., 1990, "The Rocketdyne Multifunction Tester, I: Test Method," Rotordynamic Instability Problems of High Performance Turbomachinery, Proceedings of a Workshop held at Texas A&M University.

Rouvas, C., and D. Childs, 1993, "A Parameter Identification Method for the Rotordynamic Coefficients of a High Speed Reynolds Number Hydrostatic Bearing," ASME *Journal of Vibration and Acoustics,* Vol. 115, pp. 264-270.

Instrumental Variable Filter Method

Fritzen, C. P., 1985, "Identification of Mass, Damping, and Stiffness Matrices of Mechanical Systems," ASME Paper 85-DET-91.

Massmann, H., and R. Nordmann, 1985, "Some New Results Concerning the Dynamic Behavior of Annular Turbulent Seals," Rotordynamic Instability Problems of High Performance Turbomachinery, Proceedings of a workshop held at Texas A&M University, Dec, pp. 179-194.

Diaz, S., and L. San Andrés, 1999, "A Method for Identification of Bearing Force Coefficients and its Application to a Squeeze Film Damper with a Bubbly Lubricant," STLE Tribology Transactions, Vol. 42, 4, pp. 739-746.

Field methods for In-Situ Parameter Identification

De Santiago, O., and L., San Andrés, 2004, "Identification of Bearing Force Coefficients from Measurements of Imbalance Response of a Flexible Rotor", ASME Paper GT 2004-54160

De Santiago, O., and L., San Andrés, 2004, "Identification of Bearing Force Coefficients in Flexible Rotor Systems", Eighth International Conference on Vibrations in Rotating Machinery, September 7th to 9th, 2004, University of Wales, Swansea, Wales, UK

De Santiago, O., and L., San Andrés, 2007, "Experimental Identification of Bearing Dynamic Force Coefficients in a Flexible Rotor – Further Developments," *Tribology Transactions,* v. 50(1), p. 114-126. Editor's Choice – Tribology & Lubrication Technology, June 2007, pp. 40-50.

De Santiago, O.C., and San Andrés, L., 2007, "Field Methods for Identification of Bearing Support Parameters-Part I: Identification from Transient Rotor Dynamic Response due to Impacts," ASME J. Eng. Gas Turbines Power, **129**, pp. 205-212.

De Santiago, O.C., and San Andrés, L., 2007, "Field Methods for Identification of Bearing Support Parameters-Part II: Identification from Rotor Dynamic Response due to Imbalances," ASME J. Eng. Gas Turbines Power, **129**, pp. 213-219.

Nonlinear-Linear System Parameter Identification

Rice, H.J., and Fitzpatrick, J.A., 1991, "Procedure for the Identification of Linear and Non-Linear Multi-Degree-of-Freedom Systems," J. Sound Vib., **149**(3), pp. 397-411

San Andrés, L., and Delgado, A., 2007, "Identification of Force Coefficients in a Squeeze Film Damper with a Mechanical End Seal- Centered Circular Orbit Tests," ASME J. Tribol., **129**(3), pp. 660-668.

Delgado, A., and San Andrés, L., 2008, "Nonlinear Identification of Mechanical Parameters in a Squeeze Film Damper with Integral Mechanical Seal," ASME paper No. GT2008-50528. (Scheduled for publication in J. Eng. Gas Turbines Power, September 2009, vol. 131)

Delgado, D., and San Andrés, L., 2009, "Identification of Squeeze Film Damper Force Coefficients from Multiple-Frequency, Non-Circular Journal Motions," ASME paper No**.** GT2009-59175(Scheduled for publication in J. Eng. Gas Turbines Power, 2010, vol. 132)

NOTES 14.
A METHOD FOR IDENTIFICATION OF BEARING FORCE COEFFICIENTS AND ITS APPLICATION TO A SQUEEZE FILM DAMPER WITH A BUBBLY LUBRICANT

Reproduced with permission from: **Sergio E. Diaz, Luis A. San Andrés, STLE Tribology Transactions, Vol. 42, 4, pp. 739-746, 1999**

ABSTRACT

A general formulation of the instrumental variable filter (*IVF*) method for parameter identification of a *n*-DOF (Degrees Of Freedom) mechanical linear system is presented. The *IVF* is a frequency domain method and an iterative variation of the least-squares approximation to the system flexibilities. Weight functions constructed with the estimated flexibilities are introduced to reduce the effect of noise in the measurements, thus improving the estimation of dynamic force coefficients. The *IVF* method is applied in conjunction to impact force excitations to estimate the mass, stiffness, and damping coefficients of a test rotor supported on a squeeze film damper (*SFD*) operating with a bubbly lubricant. The amount of air in the lubricant is varied from nil to 100% to simulate increasing degrees of severity of air entrainment into the damper film lands. The experimental results and parameter estimation technique show that the *SFD* damping force coefficients increase as the air volume fraction in the mixture increases to about 50% in volume content. The damping coefficients decrease rapidly for mixtures with larger air concentrations. The unexpected increase in direct damping coefficients indicates the complexity of the *SFD* bubbly flow field and warrants further experimental verification.

NOMENCLATURE

$\boldsymbol{A}$	Matrix of coefficients for error equation [2*nN*,3*n*].	K_{ij}	Equivalent stiffness coefficients of *SFD*-rotor system [N/m].
c	*SFD* nominal radial clearance [0.290 mm].	l	Shaft length [304.8 mm].
$\boldsymbol{C}$	Matrix of damping coefficients [*n*x*n*].	L	Journal length [25.4 mm].
C_{ij}	Equivalent damping coefficients of *SFD*-rotor system[Nsec/m].	m	Iteration counter for *IVF* method.
		$\boldsymbol{M}$	Matrix of inertia coefficients [*n*,*n*].
d	Shaft diameter [9.5 mm].	M_{ij}	Equivalent inertia coefficients of *SFD*-rotor system [kg].
D	Journal diameter [50.8 mm].		
$\boldsymbol{E}$	Error matrix [*n*,*n*].	n	Number of degrees of freedom of the system.
$\bar{\boldsymbol{E}}$	***E***xtended error matrix [2*nN*,*n*].	N	Number of frequencies considered for identification range.
$\boldsymbol{f}$	Forcing vector [*n*].		
$\boldsymbol{F}$	DFT of the force vector $\boldsymbol{f}$ [*n*].	t	Time [sec].
$\underline{\boldsymbol{F}}$	Flexibility matrix [*n*,*n*].	$\boldsymbol{W}$	Weight matrix for IV method [2*nN*,3*n*].
$\underline{\boldsymbol{H}}$	Impedance matrix [*n*,*n*]	x	Displacements (state) vector [*n*].
$\boldsymbol{i}$	Imaginary unit [√-1].	$\boldsymbol{X}$	DFT of the displacement vector $\boldsymbol{x}$ [*n*].
$\boldsymbol{I}$	Identity matrix [*n*,*n*].	X, Y	Horizontal and vertical coordinates, respectively.
$\bar{\boldsymbol{I}}$	Extended identity matrix [2*nN*,*n*].	μ	Fluid viscosity [Pa.s].
i,j	Indexes for degrees of freedom [=1,2,...*n*].	ω	Frequency [rad/s].
k	Frequency index.	$\boldsymbol{0}$	Zero (null) matrix [*n*,*n*].

$\boldsymbol{K}$ Matrix of stiffness coefficients [n,n].

INTRODUCTION

Experimental identification of linearized bearing parameters, namely stiffness and damping force coefficients, is of importance to verify the rotordynamic performance of actual fluid film bearing elements and to validate (and calibrate) predictive tools for computation of bearing and seal dynamic forced responses. The ultimate goal is to provide reliable data bases from which to determine the confidence of bearing and/or seal operation under both normal design conditions and extreme environments due to unforeseen events. In addition, even advanced analytical models are very limited or non-existing for certain bearing and seal configurations and with stringent particular operating conditions, and thus experimental measurements of actual bearing force coefficients constitute the only option available to generate engineering results of interest. Squeeze film dampers operating with air entrainment are but an example of the many applications where systematic experimentation becomes mandatory.

The estimation of bearing and seal rotordynamic force coefficients has been traditionally based on time domain response procedures [1]. However, these techniques are limited in their scope, use only a limited amount of the recorded information, and often provide poor results with marginal confidence levels [2]. Modern bearing parameter identification techniques are based on frequency domain procedures, where dynamic force coefficients are estimated from transfer functions of measured displacements (velocities and accelerations as well) due to external loads of a prescribed time varying structure. The frequency domain methods take advantage of high speed computing and processors, thus producing estimates of system parameters in real time and at a fraction of the cost (and effort) prevalent with cumbersome time domain techniques [3, 4, 5].

This paper presents a frequency domain method for identification of linearized bearing force coefficients from test fluid film bearing elements. The technique, a variation of a least square estimator, is based on the Instrumental Variable Filter (*IVF*) Method with the capability to automatically reduce the noise inherent in any measurement and to provide reliable bearing force coefficients within a frequency range. The analysis introduces the equations of motion for the test system and the measurement of time domain responses. The description follows with the transformation of displacement and load dynamic responses to the frequency domain, and the implementation of the procedure for error minimization and curve fitting of the (output/input) transfer functions over a selected frequency range.

The identification method is applied to the estimation of system force coefficients $\{K_{ij}, C_{ij}, M_{ij}\}_{ij=X,Y}$ for a small test rotor supported on a squeeze film damper (*SFD*). Calibrated impact guns excite the rotor in two radial planes *(X,Y)* and the rotor displacements are recorded for a multiple sequence of impacts. The *SFD* operates with an air in oil (bubbly) mixture to simulate prevalent operating conditions with air entrainment [6]. The identification procedure also renders dry, i.e. without lubricant, structural force coefficients.

INSTRUMENTAL VARIABLE PARAMETER IDENTIFICATION TECHNIQUE

Consider a *n-degree of freedom* linear mechanical system governed by the following system of differential equations.

$$\boldsymbol{M}\,\ddot{\boldsymbol{x}}_{(t)} + \boldsymbol{C}\dot{\boldsymbol{x}}_{(t)} + \boldsymbol{K}\boldsymbol{x}_{(t)} = \boldsymbol{f}_{(t)} \qquad (1)$$

where $\boldsymbol{f}_{(t)}$ and $\boldsymbol{x}_{(t)}$ represent the external forcing function and system displacements, respectively. The $(\dot{\cdot})$ denotes differentiation with respect to time. The square matrices $\boldsymbol{M}$, $\boldsymbol{K}$ and $\boldsymbol{C}$ contain the generalized mass, stiffness and damping force coefficients representing the parameters of the system. The objective of the identification procedure is to determine the system force coefficients from measurements of the system dynamic response due to applied external loads. The governing equations can be written in the frequency domain as

$$\left[-\omega^2\boldsymbol{M} + \boldsymbol{i}\omega\boldsymbol{C} + \boldsymbol{K}\right]\boldsymbol{X}_{(\omega)} = \underline{\boldsymbol{H}}_{(\omega)}\boldsymbol{X}_{(\omega)} = \boldsymbol{F}_{(\omega)} \qquad (2)$$

where $\boldsymbol{X}_{(\omega)}$ and $\boldsymbol{F}_{(\omega)}$ are the discrete Fourier transforms (DFT) of the time varying forces and displacements, $\boldsymbol{f}_{(t)}$ and $\boldsymbol{x}_{(t)}$, respectively. The impedance of the system is generally defined as

$$\underline{\boldsymbol{H}}_{(\omega)} = \left[-\omega^2\boldsymbol{M} + \boldsymbol{i}\omega\boldsymbol{C} + \boldsymbol{K}\right];\ \boldsymbol{i} = \sqrt{-1} \qquad (3)$$

The n^2 impedance coefficients $\{\underline{\boldsymbol{H}}_{i,j}\}_{i,j=1,\ldots n}$ are complex algebraic functions of the excitation frequency (ω). However, the system of equations (2) provides n equations for n^2 unknowns. A n-DOF (Degrees Of Freedom) system has n-linearly independent modes of vibration. Thus, n-linearly independent excitations $\{\boldsymbol{F}^i\}_{i=1,\ldots n}$ should lead to n-linearly independent responses $\{\boldsymbol{X}^i\}_{i=1,\ldots n}$, hence rendering n-linearly independent systems of equations of the form (2) for any given excitation frequency. The selection of the set of force excitations depends fundamentally on the structure and constraints of the system. A typical method consists of exciting the system at the location of each degree of freedom, one at the time[1]. However, any combination of forcing functions is appropriate as long as the n-forces are linearly independent.

The n-systems of equations (2) representing the independent measurements can be regrouped in the following form,

$$\underline{\boldsymbol{H}}_{(\omega)}\left[\boldsymbol{X}^1_{(\omega)} \,\vdots\, \boldsymbol{X}^2_{(\omega)} \,\vdots\, \cdots \,\vdots\, \boldsymbol{X}^n_{(\omega)}\right] = \left[\boldsymbol{F}^1_{(\omega)} \,\vdots\, \boldsymbol{F}^2_{(\omega)} \,\vdots\, \cdots \,\vdots\, \boldsymbol{F}^n_{(\omega)}\right] \qquad (4)$$

and the system impedance coefficients at the frequency of interest can be computed from

$$\underline{\boldsymbol{H}}_{(\omega)} = \left[\boldsymbol{F}^1_{(\omega)} \,\vdots\, \boldsymbol{F}^2_{(\omega)} \,\vdots\, \cdots \,\vdots\, \boldsymbol{F}^n_{(\omega)}\right]\left[\boldsymbol{X}^1_{(\omega)} \,\vdots\, \boldsymbol{X}^2_{(\omega)} \,\vdots\, \cdots \,\vdots\, \boldsymbol{X}^n_{(\omega)}\right]^{-1} \qquad (5)$$

---

[1] Note that this procedure when carried out with static loads leads naturally to the determination of the system flexibilities, i.e. the influence coefficient method.

The definition of the impedance coefficients, equation (3), renders a quadratic relationship in frequency. To identify the force coefficients it is sufficient, in principle, to obtain the impedance coefficients at three different and well spaced frequencies and then use some curve-fit procedure to extract the force coefficients $(M_{i,j},\ C_{i,j},\ K_{i,j})_{i,j=1,2,\ldots,n}$. Note that the model assumes the force coefficients or system parameters are constants independent of frequency. In the following, the basic issues related to the selection of appropriate test frequencies are discussed.

In a linear system excited by a sustained time varying force, the system response has the same frequency content as the external excitation as long as the transient motions not due to the external force have died out. Therefore, in an ideal case only pure-tone forced excitations are required, and response measurements conducted at only three different excitation frequencies should be sufficient to fully determine the system physical parameters. In practice, however, measurements of forces and displacements contain noise that affects greatly the desired results. In some other cases, the objective is to find linearized force coefficients that represent the behavior of a certain non-linear system over a frequency range. In both circumstances, whether dealing with measurement noise or localized system linearization, the identification procedure leads to a problem where the minimization of errors is of importance.

Instead of working with the minimum amount of frequencies needed, it is best to obtain measurements for a whole set of frequencies within a range of interest. However, an increased cost (and time) in the experimental procedure is the natural consequence if the measurements are conducted with a pure tone force excitation for every frequency of interest. Therefore, other forms of force excitations must be sought. The two excitations most commonly used are the impact load and the multi-harmonic force, though the sweep sine force is also often employed [7].

The fundamental idea is to excite the system with a wide-band-spectrum force which will result in a wide-band system frequency response. The application of the DFT to the measured forces and displacements leads to discrete algebraic equations in the frequency domain and at the selected, say N, frequencies within the range of interest. The k^{th} impedance coefficients at the frequency (ω_k) could then be found from:

$$\underline{\mathbf{H}}^{k} = \left[\mathbf{F}^{1}_{(\omega_k)} \;\vdots\; \mathbf{F}^{2}_{(\omega_k)} \;\vdots\; \cdots \;\vdots\; \mathbf{F}^{n}_{(\omega_k)}\right]\left[\mathbf{X}^{1}_{(\omega_k)} \;\vdots\; \mathbf{X}^{2}_{(\omega_k)} \;\vdots\; \cdots \;\vdots\; \mathbf{X}^{n}_{(\omega_k)}\right]^{-1} \qquad k = 1,2,\ldots,N \tag{6}$$

From here on, several paths could be followed to determine the $3n^2$ parameters $(M_{i,j},\ C_{i,j},\ K_{i,j})_{i,j=1,2,\ldots,n}$ from the n^2 impedance coefficients, $(\underline{\boldsymbol{H}}_{i,j})_{i,j=1,2,\ldots,n}$, as functions of the excitation frequency. The most direct and most commonly used procedure consists of performing independent least-squares curve fittings to the real and imaginary parts of each component of the impedance matrix $\underline{\boldsymbol{H}}$ over a range of frequencies. This procedure takes advantage of the fact that each system coefficient, $(M_{i,j},\ C_{i,j},\ K_{i,j})$, appears only in one impedance term making the polynomial curve fit (quadratic for the real part and linear for the imaginary part) independent of each other.

However, the direct least-squares curve fit of the system impedances is highly sensitive to the level of the inherent noise in the measurements and to the selection of the frequency range for the approximation [8]. A more robust method is achieved based on the following identity [4]

$$\underline{\boldsymbol{F}}^{k}\,\underline{\boldsymbol{H}}_{(\omega_k)} = \boldsymbol{I} + \boldsymbol{E}^{k} \tag{7}$$

where $\underline{\boldsymbol{F}}^{k}$ represents the measured flexibility matrix, defined as the inverse of the impedance $\underline{\boldsymbol{H}}^{k}$, equation (6), at the frequency ω_k. $\underline{\boldsymbol{H}}$ in the equation above corresponds to the estimated system impedance as defined by equation (3). $\boldsymbol{E}^{k}$ is the matrix of errors due to the approximation. In this formulation, the flexibility coefficients work as weight functions of the errors in the minimization procedure. Whenever the flexibility coefficients are large, the error is also penalized by a larger value. As a result, the minimization procedure will become better in the neighborhood of the system resonances (natural frequencies) where the dynamic flexibilities are maximums (i.e., null dynamic stiffness, K-$\omega^2 M$). That is, the measurements containing resonance regions will have more weight on the fitted system parameters. This result is of importance since forcing functions exciting the system resonances are more reliable since this is more sensitive at those frequencies, and the measurements are accomplished with larger signal to noise ratios. In addition, it is precisely around the resonant frequencies where all the physical parameters (mass, damping and stiffness) most affect appreciably the system response. For "too low" frequencies the important parameter is the stiffness, while for "too high" frequencies the inertia dominates the response. Only near the resonance do all three parameters have an important effect on the system response. Therefore, it is more convenient to minimize the approximation errors using equation (7) rather than directly curve fitting the impedances. However, this last procedure could be rather intricate. The approximation functions on the left-hand-side of equation (7) are no longer independent of each other since all the parameters appear in all of them. This difficulty is easily overcome by rearranging the impedance definition (3) to the form

$$\underline{\boldsymbol{H}}_{(\omega)} = \left[-\omega^2 \boldsymbol{I} \;\vdots\; \boldsymbol{i}\;\; \omega \boldsymbol{I} \;\vdots\; \boldsymbol{I} \right] \begin{bmatrix} \boldsymbol{M} \\ \boldsymbol{C} \\ \boldsymbol{K} \end{bmatrix} \tag{8}$$

Substituting the definition (8) into equation (7) and separating into real and imaginary parts gives

$$\begin{bmatrix} Re\left(\boldsymbol{F}^k \left[-\omega_k{}^2 \boldsymbol{I} \;\vdots\; \boldsymbol{i}\omega_k \boldsymbol{I} \;\vdots\; \boldsymbol{I} \right]\right) \\ Im\left(\boldsymbol{F}^k \left[-\omega_k{}^2 \boldsymbol{I} \;\vdots\; \boldsymbol{i}\omega_k \boldsymbol{I} \;\vdots\; \boldsymbol{I} \right]\right) \end{bmatrix} \begin{bmatrix} \boldsymbol{M} \\ \boldsymbol{C} \\ \boldsymbol{K} \end{bmatrix} = \begin{bmatrix} \boldsymbol{I} \\ \boldsymbol{0} \end{bmatrix} + \begin{bmatrix} Re\left(\boldsymbol{E}^k\right) \\ Im\left(\boldsymbol{E}^k\right) \end{bmatrix} \tag{9}$$

Stacking the equations for the N discrete frequencies at which the identification procedure is to be performed renders

$$\boldsymbol{A} \begin{bmatrix} \boldsymbol{M} \\ \boldsymbol{C} \\ \boldsymbol{K} \end{bmatrix} = \bar{\boldsymbol{I}} + \bar{\boldsymbol{E}} \tag{10}$$

where

$$\boldsymbol{A}=\begin{bmatrix} \begin{bmatrix} Re\left(\underline{\boldsymbol{F}}^{1}\left[-\omega_1{}^2\boldsymbol{I} \;\vdots\; \boldsymbol{i}\omega_1\boldsymbol{I} \;\vdots\; \boldsymbol{I}\right]\right) \\ Im\left(\underline{\boldsymbol{F}}^{1}\left[-\omega_1{}^2\boldsymbol{I} \;\vdots\; \boldsymbol{i}\omega_1\boldsymbol{I}\right] \;\vdots\; \boldsymbol{I}\right]\right) \end{bmatrix} \\ \vdots \\ \begin{bmatrix} Re\left(\underline{\boldsymbol{F}}^{N}\left[-\omega_N{}^2\boldsymbol{I} \;\vdots\; \boldsymbol{i}\omega_N\boldsymbol{I} \;\vdots\; \boldsymbol{I}\right]\right) \\ Im\left(\underline{\boldsymbol{F}}^{N}\left[-\omega_N{}^2\boldsymbol{I} \;\vdots\; \boldsymbol{i}\omega_N\boldsymbol{I} \;\vdots\; \boldsymbol{I}\right]\right) \end{bmatrix} \end{bmatrix} \qquad \bar{\boldsymbol{I}}=\begin{bmatrix} \boldsymbol{I} \\ \boldsymbol{0} \\ \vdots \\ \boldsymbol{I} \\ \boldsymbol{0} \end{bmatrix} \quad \bar{\boldsymbol{E}}=\begin{bmatrix} \begin{bmatrix} Re\left(\boldsymbol{E}^{1}\right) \\ Im\left(\boldsymbol{E}^{1}\right) \end{bmatrix} \\ \vdots \\ \begin{bmatrix} Re\left(\boldsymbol{E}^{N}\right) \\ Im\left(\boldsymbol{E}^{N}\right) \end{bmatrix} \end{bmatrix}$$

Fritzen [3] introduces the elegant Instrumental Variable Filter Method (*IVF*) to compute the system coefficients that minimize the Euclidean (L^2) norm of the global error matrix $\bar{\boldsymbol{E}}$. This procedure was originally developed to estimate parameters in econometry problems. Massmann and Nordmann [4] have applied the method to fluid film seal elements. The *IFV* method proposes a solution of the form

$$\begin{bmatrix} \boldsymbol{M} \\ \boldsymbol{C} \\ \boldsymbol{K} \end{bmatrix}^{m+1} = \left(\left[\boldsymbol{W}^{m}\right]^{T}\boldsymbol{A}\right)^{-1}\left[\boldsymbol{W}^{m}\right]^{T}\bar{\boldsymbol{I}} \tag{11}$$

The weight matrix $\boldsymbol{W}$ is chosen to have the same form as $\boldsymbol{A}$, see equation (10), but it consists of the analytical flexibilities rather than the measured ones, i.e.,

$$\boldsymbol{W}^{m}=\begin{bmatrix} \begin{bmatrix} Re\left(\underline{\boldsymbol{F}}^{m}_{(\omega_1)}\left[-\omega_1{}^2\boldsymbol{I} \;\vdots\; \boldsymbol{i}\omega_1\boldsymbol{I} \;\vdots\; \boldsymbol{I}\right]\right) \\ Im\left(\underline{\boldsymbol{F}}^{m}_{(\omega_1)}\left[-\omega_1{}^2\boldsymbol{I} \;\vdots\; \boldsymbol{i}\omega_1\boldsymbol{I} \;\vdots\; \boldsymbol{I}\right]\right) \end{bmatrix} \\ \vdots \\ \begin{bmatrix} Re\left(\underline{\boldsymbol{F}}^{m}_{(\omega_N)}\left[-\omega_N{}^2\boldsymbol{I} \;\vdots\; \boldsymbol{i}\omega_N\boldsymbol{I} \;\vdots\; \boldsymbol{I}\right]\right) \\ Im\left(\underline{\boldsymbol{F}}^{m}_{(\omega_N)}\left[-\omega_N{}^2\boldsymbol{I} \;\vdots\; \boldsymbol{i}\omega_N\boldsymbol{I} \;\vdots\; \boldsymbol{I}\right]\right) \end{bmatrix} \end{bmatrix} \tag{12}$$

where

$$\underline{\boldsymbol{F}}^{m}_{(\omega)}=\left[\left[-\omega^2\boldsymbol{I} \;\vdots\; \boldsymbol{i}\omega\boldsymbol{I} \;\vdots\; \boldsymbol{I}\right]\begin{bmatrix} \boldsymbol{M} \\ \boldsymbol{C} \\ \boldsymbol{K} \end{bmatrix}^{m}\right]^{-1} \tag{13}$$

A first iteration (m=1) is performed with $\boldsymbol{W} = \boldsymbol{A}$, which corresponds to the standard least-squares solution of the problem in equation (10). Then equation (11) is applied iteratively until a given convergence criterion is satisfied. This criterion can be conveniently chosen depending on the desired results. For example, the square summation of the differences between the parameters at iteration m and (m-1) can be required to be less than a certain value, i.e. limiting the Euclidean norm of the error. Alternatively, it can be required that the largest difference be less than the largest acceptable error, i.e. limiting the L_1 norm of the error. Different tolerances to each variable could also be asserted depending on their physical units and significance. It is clear that the substitution of $\boldsymbol{W}$ for the discrete measured flexibility $\boldsymbol{A}$ (which also contains noise) improves the prediction of the

system parameters. Note that the product $\boldsymbol{A}^T\boldsymbol{A}$ amplifies the noisy components and adds them. Therefore, even if the noise has a zero mean value, the addition of its squares becomes positive resulting in a bias error. On the other hand, $\boldsymbol{W}$ does not have components correlated to the measurement noise. That is, no bias error is kept in the product $\boldsymbol{W}^T\boldsymbol{A}$. Consequently, the approximation to the system parameters is improved.

An example of the application of the *IVF* parameter identification method to a simple laboratory rotor-bearing system follows. Ransom, et al. [9] provides a successful application for the identification of force coefficients in multiple-pocket gas damper seals.

SFDs AND AIR ENTRAINMENT

Squeeze film dampers (*SFDs*) are effective means to introduce damping to rotor-bearing systems thus reducing vibration amplitudes at critical speeds and improving system stability. A *SFD* is a type of hydrodynamic bearing in which a non-rotating journal whirls with the shaft and squeezes a thin film of lubricant that surrounds it. The squeezing action generates hydrodynamic pressures yielding a force that opposes the journal motion and provides the desired damping. Generally, *SFDs* operate with low levels of external pressurization and are open to ambient on the sides. Under these conditions, the cyclic squeezing in and out of the oil results in the entrapment of external air and leads to the formation of a bubbly (foam-like) mixture of air and oil within the film [10,11]. The mixture has different material properties than the pure lubricant, and consequently it affects considerably the dynamic force performance of the *SFD*. Zeidan, et al. [12] estimate damping coefficient losses as large as 75% of the value predicted for operation with pure oil.

The phenomenon of air entrainment is readily acknowledged to be the main obstacle for the reliable prediction of *SFD* dynamic forces [13]. Yet no accurate measurements correlating the viscous damping coefficients to the amount of entrained air are available. The lack of firm (quantifiable) experimental evidence prevents further advances in the theoretical formulation of SFD flows [14, 15].

EXPERIMENTAL FACILITY

Figure 1 shows a section of the test rig and the instrumentation setup for force and displacements measurement. The shaft of length 305 mm (12") and diameter 9.5 mm (3/8") is supported by a bronze bushing at the drive end and by a squeeze film damper at the rotor midspan. The squeeze film damper consists of a steel journal of diameter *(D)* and length *(L)* equal to 50.8 mm and 25.4 mm, respectively, and a Plexiglas transparent housing. The damper radial clearance *(c)* is 0.29 mm (11.4 mils). Four flexible rods compose the squirrel cage that supports the damper journal. A ball bearing inside the *SFD* journal forces the shaft and the journal to whirl together while allowing the shaft to rotate. A flexible coupling transmits torque from the DC drive motor but isolates lateral vibration. A massive disk is mounted on the free end of the shaft to provide inertia and a location to install imbalance masses.

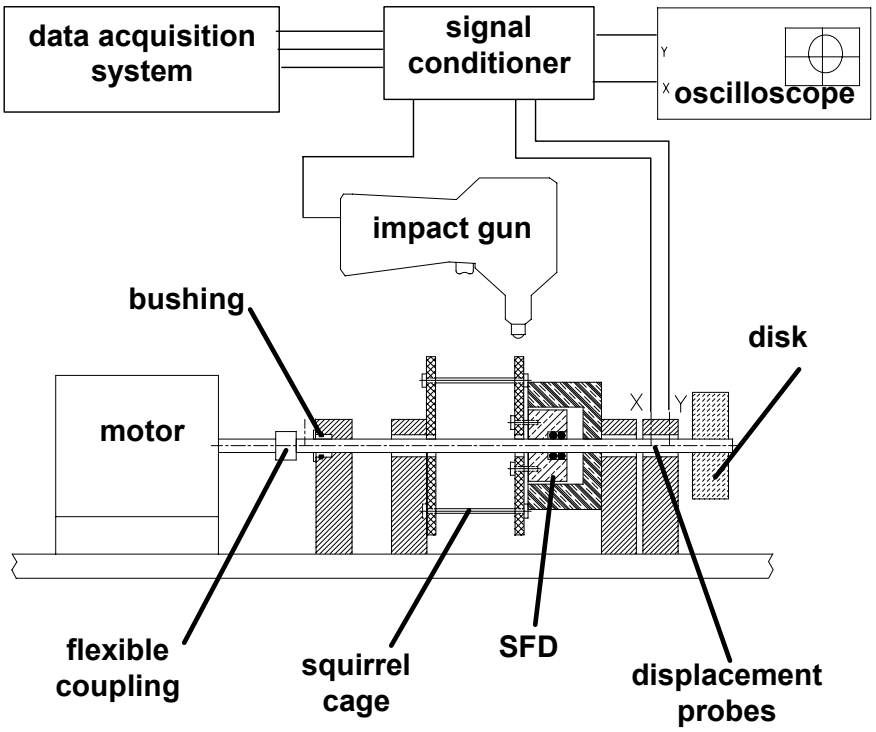

Fig. 1-Test rig section and instrumentation

Two eddy current proximity sensors measuring horizontal and vertical shaft displacements are installed at (L_X) 213 mm and (L_Y) 254 mm from the rotor drive end, respectively. The *SFD* and disk centers are located at (L_{SFD}) 151 mm and (L_D) 274 mm from the rotor drive end, respectively. The bushing stiffness is larger than the *SFD* elastic support stiffness, and thus the rotor pivots about the bushing location for rotor speeds below 6,000 rpm as shown in Figure 2. For the range of frequencies of interest, the rotor can be considered as an equivalent point mass system with two degrees of freedom in the lateral directions *(X,Y)*.

A controlled mixture of air and ISO VG 2 oil flows to the *SFD* through a small hole located at the top of the bearing housing. The viscosity (μ) of the pure lubricant is 2.25 centipoise at a temperature of 30^o C. The lubricant exits the test section through both sides of the damper which are open to ambient. The mixture is generated in a sparger element installed at the connection of the air and oil lines. The proportions of air and oil are accurately regulated with valves on each feed line. The air volume fraction is computed as the ratio of measured air volumetric flow rate to total (air + oil) volumetric flow rate.

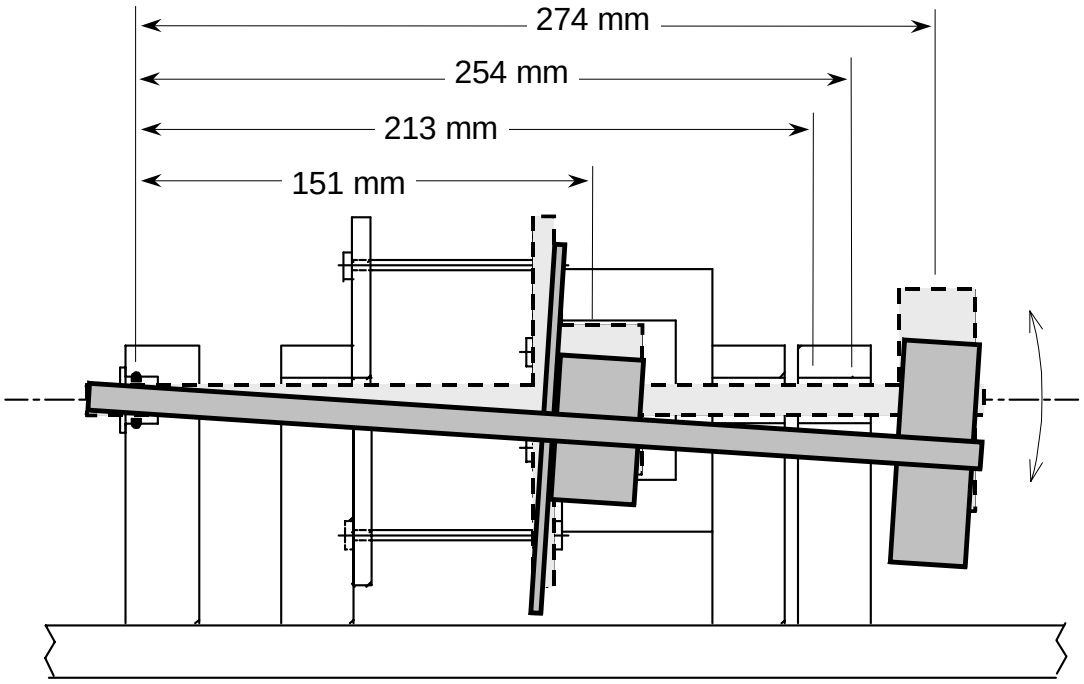

Fig. 2-Conical mode shape of the rotor

An instrumented impact gun excites the rotor shaft at the location of the *SFD*. A support allows installation of the impact gun for excitations in the horizontal and vertical directions. An A/D board and computer record the time traces of the impact force and the shaft lateral displacements simultaneously at a rate of 6,700 samples per second for 1.2 seconds. All tests are performed without rotor spinning.

EXPERIMENTAL PROCEDURE

The rotor is carefully centered within the damper clearance and the valves in the oil and air feed lines are set to the desired mixture composition. The air and oil flow rates as well as the values of supply pressures and temperature are recorded for the computation of the air volume fraction. The system fundamental natural frequencies, measured by impact tests under dry conditions, are equal to 28.4 Hz and 30.1 Hz in the horizontal and vertical directions, respectively. The difference is due to asymmetry in the squirrel cage stiffness as demonstrated earlier by static load measurements of the system flexibility [15].

The test system has two DOF (n=2). Thus, two independent excitations are required to compute all four coefficients of the impedance matrix $\underline{\boldsymbol{H}}$. Impact loads in the horizontal (X) and vertical (Y) directions are sufficient to perform the identification procedure. Eight impacts are exerted on each direction for every mixture condition, and the time traces of forces and displacements are stored. The impact forces are applied at the *SFD* journal and the shaft displacements are measured near the end disk. Equivalent X and Y displacements at the *SFD* location are computed using the conical mode of motion with a pivot at the bushing as depicted in Figure 2. A DFT transform is applied to the dynamic displacements and loads, and the resulting spectra are regrouped into eight sets, each one containing the data from the X and Y impacts. Equation (6) is then employed to compute the

impedance elements ($\underline{H}_{XX}$, $\underline{H}_{XY}$, $\underline{H}_{YX}$, $\underline{H}_{YY}$) for each data set at the discrete values of frequency. Then, the eight discrete functions corresponding to each impedance coefficient are averaged to render a single frequency function in which the noise not related to the load excitation is reduced[2]. Figure 3 shows typical time variations of the applied force and displacement responses, and their corresponding DFTs for one case of impact excitation in the *X* direction. The measurements include a short pre-trigger and contain the full span of the transient motions, thus avoiding "leaking" effects on the DFT transforms. Figure 3 also shows the excitation to have a wide-band spectrum that covers the whole range of frequencies of interest.

The *IVF* parameter identification method, equation (11), is applied to the averaged flexibilities over a selected range of frequencies around the fundamental natural frequency of the system. In this case, the selected range goes from 8.1 Hz to 48.8 Hz and includes the peak response (resonance) region. The process is repeated for six different lubricant mixture compositions ranging from pure oil to 100% air. The *IVF* identification process renders estimates for the system force coefficients (M_{ij}, C_{ij}, and K_{ij})$_{i,j=X,Y}$ as functions of the air volume content in the mixture. These are equivalent system parameters referred to the location of the *SFD* middle plane.

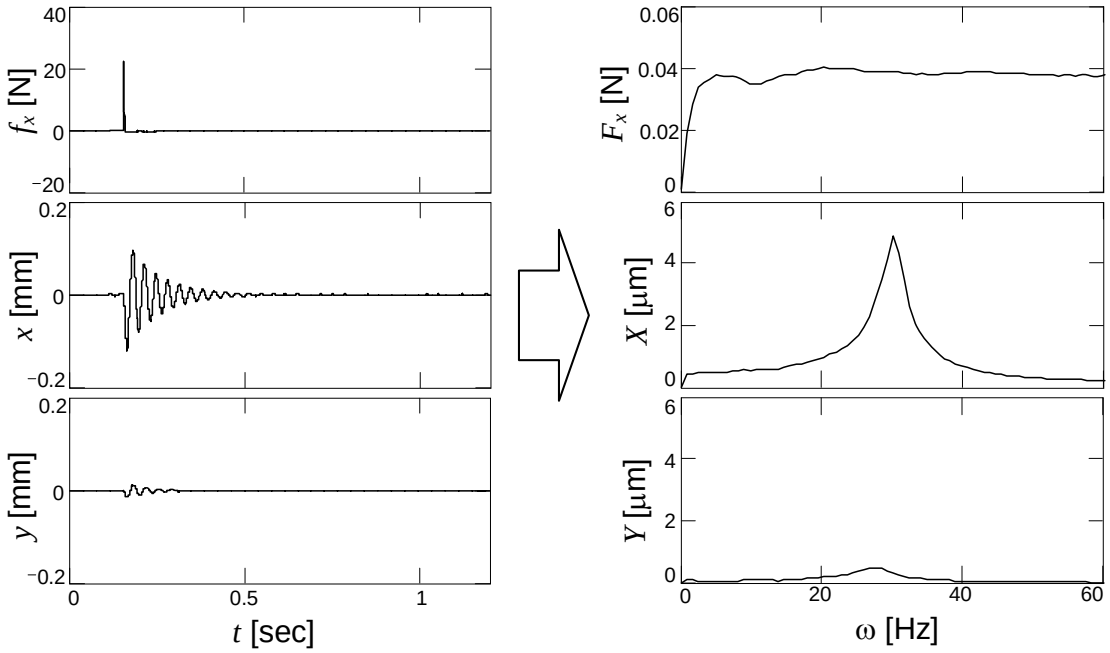

Fig. 3-Typical impact excitation in the X direction and response displacements (X and Y) in time and frequency domains

[2] Note that using the average of the impedance and/or flexibility (transfer) functions, instead of computing the transfer function from frequency averaged responses and excitations, eliminates the requirement for repetitive excitations thus allowing for the use of hand-held impact hammers or the combination of different types of excitations.

TEST RESULTS

Figure 4 depicts with symbols the flexibilities $(\underline{F}_{ij},)_{i,j=X,Y}$ measured for an air/oil mixture volume content of 8.6% as a function of the excitation frequency. The continuous lines represent the flexibilities calculated with the estimated system parameters. The experimental values represent the averages from multiple impacts as discussed before. Note that the cross-coupled flexibilities are at least one order of magnitude lower than the direct system flexibilities. Correlations between the measurements and the analytical (curve fit) functions are computed for each direct and cross-coupled flexibilities to provide a measure of the goodness of the approximation. All correlations range between 94% and 98% demonstrating the effectiveness of the *IVF* method. Furthermore, the coherence of the direct displacements to the exerted loads shows values near unity for the range of frequencies considered.

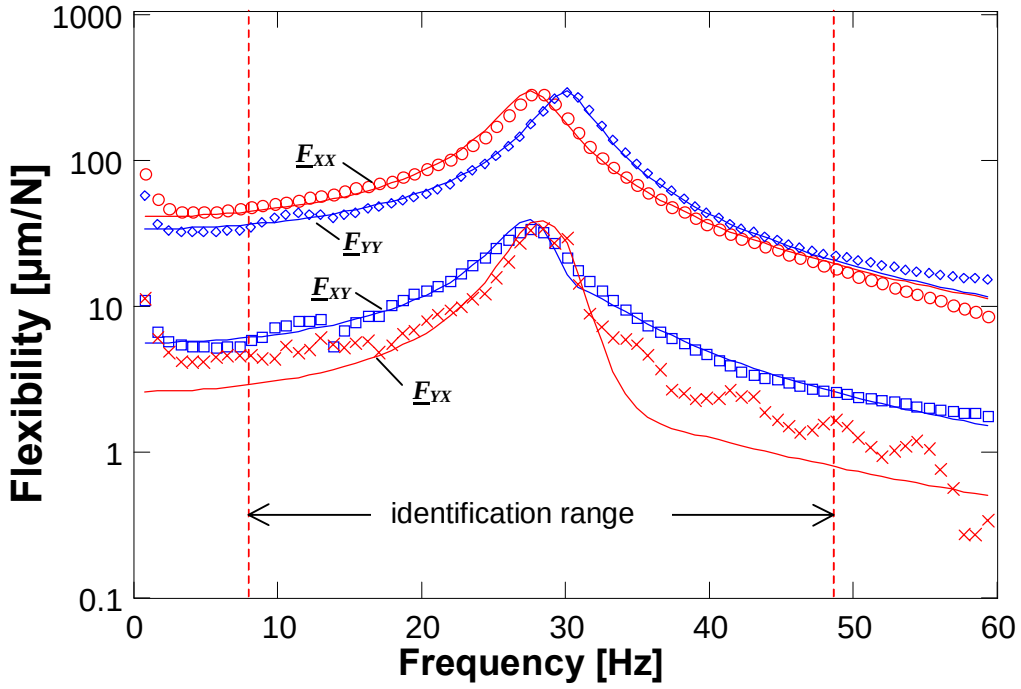

Fig. 4. Measured and approximated system flexibilities. Air volume fraction = 8.6%

Figures 5 to 7 depict the estimated dynamic force coefficients acting at the damper location. The values for an air volume fraction of one, i.e. pure air or ”dry” condition, represent solely the effect of the support structure and rotor inertia without any influence of the squeeze film. These coefficients, identified earlier by other means, serve to validate the dynamic measurement process and identification method. The direct inertia coefficients are determined by weighing the shaft, disk and journal and using simple geometrical relations to evaluate the equivalent inertia at the *SFD* location. The value calculated by this procedure is 4.02 kg, and somewhat lower than the magnitudes identified from the dynamic response tests. The direct stiffness of the elastic damper support in the horizontal direction (K_{XX}) is determined by applying static loads with a dynamometer and recording displacements with a dial gauge indicator. The measured value is K_{XX} = 150 kN/m. The equivalent structural damping is estimated from the logarithmic decrement of the dynamic response to an impact. The direct damping coefficient for no lubricant is estimated as 22.3 N.s/m.

Figure 5 shows the direct and cross-coupled inertia coefficients estimated by the *IVF* method as a function of the mixture air volume fraction. At a volume fraction of one, i.e., pure air, the *IVF* method confirms the estimations of mass coefficients performed by weighing the parts. The results also show that no significant fluid inertia is introduced by the *SFD* since the system direct inertia coefficients *(M_{XX}, M_{YY})* remain invariant when oil flows through the damper lands. The cross-coupled inertia coefficients *(M_{XY}, M_{YX})* are nearly null in all test cases.

The estimated *IVF* stiffness coefficients $\{K_{ij}\}_{i,j=X,Y}$ are depicted in Figure 6 for air volume fractions ranging from zero (pure oil) to one (pure air). The measurements for the "dry" condition confirm the static measurements of the structure characteristics. No appreciable change is observed in any of the stiffness coefficients (direct or cross-coupled) when oil is fed to the damper. The cross-coupled stiffnesses are nearly zero, though definitely negative in all tests. The vertical direct stiffness is slightly larger than the horizontal one, which agrees with the higher natural frequency measured in the vertical direction.

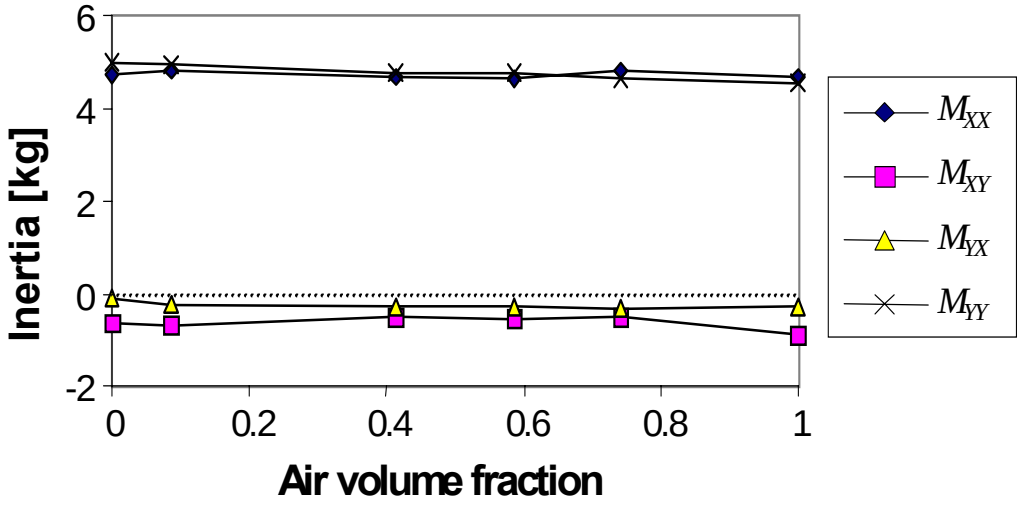

Fig. 5. Equivalent inertia coefficients vs air volume fraction.

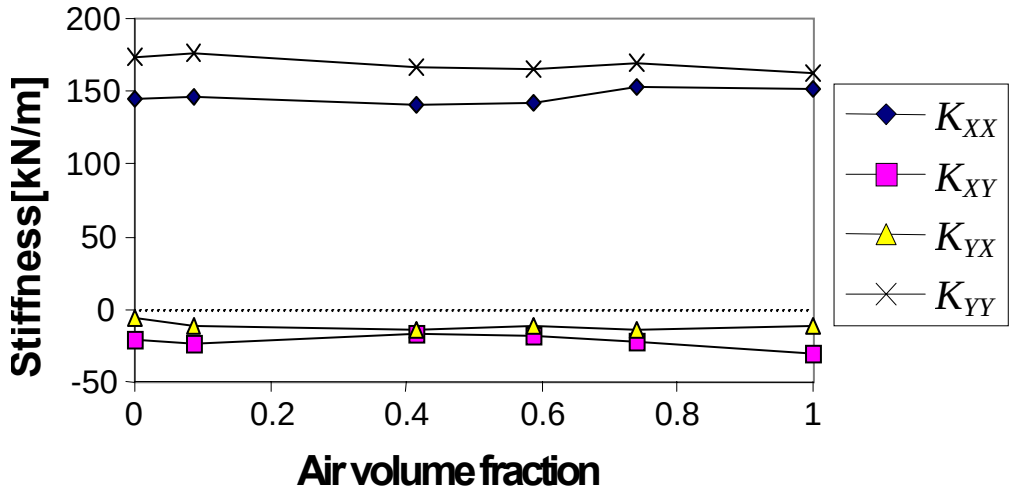

Fig. 6. Equivalent stiffness coefficients vs air volume fraction.

The average values and maximum percent variation for the stiffness and inertia force coefficients are:

K_{XX}= 146.3 kN/m (4.3%), K_{YY}= 169.1 kN/m (4.1%),

K_{XY}= 22.3 kN/m (38.7%), K_{YX}= 11.5 kN/m (24.2%),

M_{XX}= 4.7 kg (2.3%), M_{YY}= 4.8 kg (3.1%),

M_{XY}= 0.62 kg (43.4%), M_{YX}= 0.25 kg (52.4%),

Figure 7 depicts the variation of the system damping coefficients $\{C_{ij}\}_{i,j=X,Y}$ as the air volume content in the mixture increases. The measurements of the "dry" direct damping coefficients coincide with the preliminary tests based on the system logarithmic decrement. Predicted values of the *SFD* damping coefficients for the pure oil condition, centered journal and a full film extent are equal to [17]

$$C_{XX} = C_{YY} = 12\ \pi\mu R\left[\frac{L}{c}\right]^3\left(1-\frac{tgh(L/D)}{(L/D)}\right)=100\,N.s/m; \qquad C_{XY} = C_{YX} = 0 \tag{14}$$

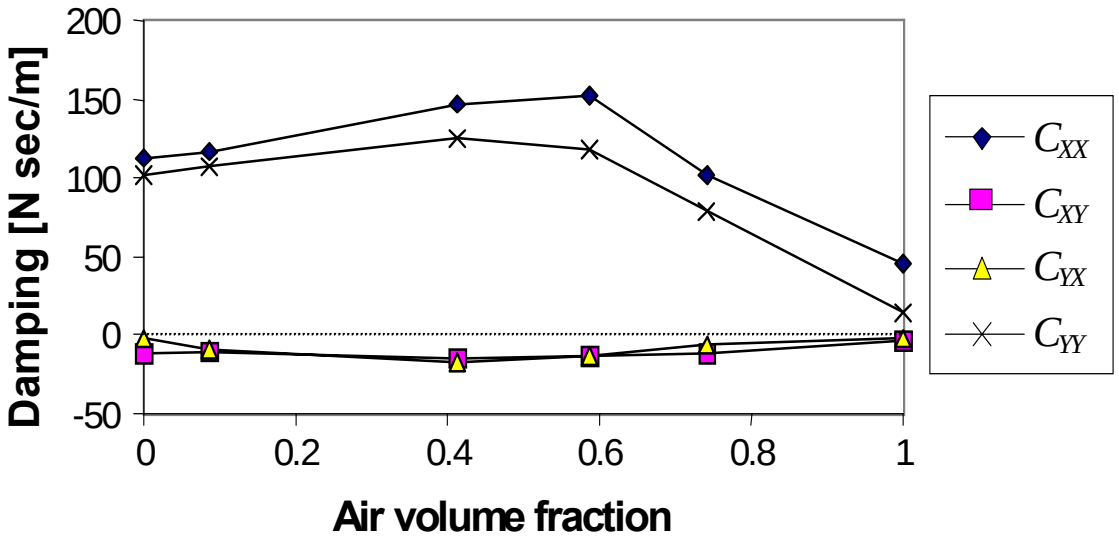

Fig. 7. Equivalent damping coefficients vs air volume fraction

These values are very close to the identified viscous damping coefficients. The estimated test cross-coupled damping coefficients are rather small, most likely within the uncertainty of the measurements. As expected, the direct damping coefficients *(C_{XX}, C_{YY})* vary significantly with the air/oil mixture composition. However, contrary to expected results, the direct damping coefficients increase steadily as the air volume fraction rises to a mixture with 50% air content. For larger concentrations of air/oil volume the direct damping coefficients decrease rapidly towards their "dry" value.

The unusual damping coefficients identified imply an increase in the effective viscosity of the lubricant mixture for small air volume contents. Chamniprasart, et al. [18] provide a fundamental analysis and limited empirical evidence verifying this phenomenon. The present authors speculate that the nature of the impact tests generates too fast system transient responses which may prevent the mixture compressibility from affecting the generation of squeeze film pressures or the overall damping coefficients. It may also be possible that, since the *SFD* is open to ambient on both sides, the air in the mixture is expelled from the film earlier than the oil, thus resulting in a lubricant with a lower air content than the one measured in the supplied mixture.

Diaz and San Andrés [8, 14, 15] detail measurements of damping coefficients in a *SFD* performing sustained circular centered orbital motions at various whirl frequencies. In these experiments, the *SFD* force coefficients steadily decrease as the air content increases in the lubricant mixture. These references reveal the complexity in the structure of bubbly flow fields and their effects on *SFD* force performance.

CONCLUSIONS

The instrumental variable filter (*IVF*) method proves a reliable tool for the identification of bearing force coefficients. The general formulation presented easily allows for extension of the method to account for support flexibility or even shaft flexibility when the equations of motion of a system need to be established experimentally. Application of the *IVF* renders the inertia, stiffness, and damping matrices of a linear system according to the selected degrees of freedom. However, the selection of the appropriate degrees of freedom is not always evident, thus representing the most critical part of the parameter identification process. The excitation force employed is also an important factor. Many options are available, but the impact force stands out because of the ease of its implementation and its wide frequency spectrum.

The *IVF* method is applied to the identification of system force coefficients in a small test rotor supported on a squeeze film damper (*SFD*) lubricated with a mixture of air in oil. The measurements show that the *SFD* does not introduce any significant amount of stiffness or inertia to the structural system. The cross-coupled damping coefficients are also negligible in all test cases. A curious trend is unveiled for the direct damping coefficients (C_{XX}, C_{YY}). Instead of a monotonic decrease for increasing air volume fractions, the direct damping coefficients increase slightly up to a lubricant composition of about 50% air in volume, where they reach a maximum. Further increase of air content reduces the damping coefficients until they reach the “dry” damping value for a pure air condition. The present results confirm that the amount of damping provided by a *SFD* is greatly affected by air entrainment. However, it is suspected that the increased viscosity for low air volume fractions will not be enough to produce an increment of the actual damping in an operating *SFD* with sustained whirl motions of significant amplitude and where the mixture compressibility effect is of utmost importance.

REFERENCES

(1) Robinson, M., Arauz, G., and San Andrés, L., "A Test Rig for the Identification of Rotordynamic Force Coefficients of Fluid Film Bearing Elements," ASME paper 95-GT-431, (1995).

(2) Ransom, D. L., "Identification of Dynamic Force Coefficients of a Labyrinth and Gas Damper Seal Using Impact Load Excitations," Master Thesis, Texas A&M University, December, (1997).

(3) Fritzen, C., "Identification of Mass, Damping, and Stiffness Matrices of Mechanical Systems," ASME paper 85-DET-91, (1985).

(4) Massmann,H., and Nordmann, R., "Some New Results Concerning the Dynamic Behavior of Annular Turbulent Seals," NASA CP 2409, Proceedings of the Instability in Rotating Machinery Workshop, Carlson City, pp. 179-194, June, (1985).

(5) Muller-Karger, C.M., and Granados, A.L., "Derivation of Hydrodynamic Bearing Coefficients Using the Minimum Square Method," ASME Journal of Tribology, 119, 4, pp. 802-807, (1997).

(6) Diaz, S. E., and San Andrés, L. A., "Measurements of Pressure in a Squeeze Film Damper with an Air/Oil Bubbly Mixture," STLE Tribology Transactions, 41, 2, pp. 282-288, (1998).

(7) Rouvas, C., "Parameter Identification of the Rotordynamic Coefficients of High-Reynolds-Number Hydrostatic Bearings," Ph.D. Dissertation, Texas A&M University, College Station, TX, May, (1993).

(8) Diaz, S. E., "Experimental Parameter Identification of a *nxn* Linear System," Internal Research Progress Report, Rotordynamics Laboratory, Texas A&M University, College Station, TX, June, (1997).

(9) Ransom, D., J. Li, L. San Andrés, and J.M. Vance, "Experimental Force Coefficients for a Two-Bladed Labyrinth Seal and a Four-Pocket Damper Seal," ASME Paper 98-Trib-28 (1998).

(10) Walton, J., Walowit, J., Zorzi, E., and Schrand, J., "Experimental Observation of Cavitating Squeeze Film Dampers," ASME Journal of Tribology, 109, pp. 290-295, (1987).

(11) Zeidan, F. Y., and Vance, J. M., "Cavitation Leading to a Two Phase Fluid in a Squeeze Film Damper," STLE Tribology Transactions, 32, 1, pp. 100-104, (1989).

(12) Zeidan, F. Y., Vance, J. M., and San Andrés, L. A. "Design and Application of Squeeze Film Dampers in Rotating Machinery", Proceedings of the 25th Turbomachinery Symposium, Texas A&M University, College Station, TX, pp. 169-188, (1996).

(13) Childs, D., Turbomachinery Rotordynamics**,** John Wiley & Sons, New York, (1993).

(14) Diaz, S., and San Andrés, L., "Reduction of the Dynamic Load Capacity in a Squeeze Film Damper Operating with a Bubbly Lubricant," ASME Paper 98-GT-109, (1998).

(15) Diaz, S., and San Andrés, L., "Effects of Bubbly Flow on the Dynamic Pressure Fields of a Test Squeeze Film Damper," ASME Paper FEDSM98-5070, Proceedings of the 1998 *ASME* Fluids Engineering Division Summer Meeting, Washington, DC, June, (1998).

(16) Karstens, C. W., "Effects of Air Entrainment on the Damping Coefficients of a Squeeze Film Damper," Senior Honor Thesis, Texas A&M University, December, (1997).

(17) San Andrés, L. and Vance, J., "Effect of Fluid Inertia on Squeeze Film Damper Forces for Small Amplitude Circular Centered Motions," ASLE Transactions, 30, pp. 69-76, (1987).

(18) Chamniprasart, K., Al-Sharif, A., Rajagopal, K.R., and Szeri, A.Z., "Lubrication With Binary Mixtures: Bubbly Oil," ASME Journal of Tribology, 115, pp. 253 – 260, (1993).